ELSEVIER

Dyes and Pigments, Vol. 34, No. 2, pp. 121–132, 1997

PII: S0143-7208(96)00070-8 0143-7208/97 $17.00+0.00

Epitaxial Growth of Polycyclic Aromatic Dyes on Oriented Polyethylene Films

Katsutoshi Tanabe[a] & Makoto Shiojiri[b]

[a]Faculty of Education, Ehime University, 3-Bunkyo, Matsuyama 790, Japan
[b]Kyoto Institute of Technology, Matsugasaki, Kyoto 606, Japan

(Received 18 June 1996; accepted 18 July 1996)

ABSTRACT

In order to evaluate the molecular interaction between dye and fibre, the crystal habit, structure and epitaxy of polycyclic aromatic dyes such as 1,4,5,8-tetraaminoanthraquinone (TAA), synthesized indigo (ING) and 6,6'-dibromoindigo (DBING), vacuum-deposited on a (110)-oriented polyethylene (PE) surface, were investigated by electron microscopy and electron diffraction. It was found that the TAA crystal has lattice constants of a = *1.584 nm,* b = *0.416 nm,* c = *1.149 nm and* $\beta = 98.03°$ *of* $P2_1a$ *cell. The dyes grow in ribbons along the [010] direction with the following epitaxial relation with respect to the PE crystal:* $(001)[100]_{TAA}//(110)[001]_{PE}$, $(\bar{2}01)[010]_{ING}//(110)[110]_{PE}$ *or* $(\bar{2}01)[010]_{ING}//(110)[001]_{PE}$, *and* $(010)[100]_{DBING}//(110)[001]_{PE}$ *or* $(0\bar{1}0)[100]_{DBING}//(110)[001]_{PE}$. © *1997 Elsevier Science Ltd*

Keywords: epitaxial growth, electron microscopy, tetraaminoanthraquinone, indigo, dibromoindigo, polyethylene.

INTRODUCTION

Not many investigations have been carried out on the growth of organic compounds on polymers since Richards [1] reported the oriented overgrowth of paraffin wax crystals on cold-drawn polyethylene. Kobayashi and Takahashi [2] investigated the epitaxial growth of various polymer crystals, and found that paraffin wax and polyethylene crystals grew with epitaxy on the surfaces of drawn polyoxymethylene and grew without epitaxy on the

surfaces of drawn nylon-6, polypropylene, polyvinylalcohol and cellulose II. They also reported the overgrowth of polycaprolactone on these substrates [3,4]. Willems [5] obtained polyethylene and paraffin crystals epitaxially grown on the surface of nylon-6. Systematic experiments of the epitaxy were carried out by Kawaguchi and co-workers [6–10] using *n*-paraffins, *n*-alcohols, *n*-carboxylic acids and also isotactic polypropylene as deposits. They then described the epitaxial modes of normal long chain compounds grown on polyolefin substrates. The growth of long chain molecules on polymers was regarded as a simple model for the epitaxy of polymer on polymer, which is of practical importance for the formation of functional thin polymer films.

There are few reports on the epitaxial growth of low molecular organic compounds on the polymer substrate. We are aware only of the recent investigations by Wittmann and Smith [11] and Ueda *et al.* [12], which were concerned with the crystal growth and the orientation of molecules such as diacetylene on highly oriented polytetrafluoroethylene thin films.

The object of this paper is to describe the epitaxial growth of tetraaminoanthraquinone (TAA) on polyethylene (PE) surfaces, referring to the results of recently reported studies of indigo (ING) and dibromoindigo (DBING) [13]. TAA is used as a disperse anthraquinone dye, and ING and DBING as indigoid vat dyes. The epitaxy of these dyes on a polymer is of interest in describing the molecular interaction between the dye and fibre.

EXPERIMENTAL

A method developed by Fischer [14] was applied for the preparation of the oriented PE thin films to be used as the substrates. PE (Hizex, $n=5360$, Mitsui Petroleum; Fig. 1a) was dissolved in *p*-xylene at boiling point to make a 0.08 wt% solution. A droplet of the solution was placed on a cleaved (001) surface of a KCl crystal heated at 105°C. After evaporating off the xylene solvent, the PE film was wet-stripped from the KCl crystal and mounted on an electron microscopy grid without any supporting film. The thickness of the prepared PE films, measured with a quartz oscillator microbalance, was about 20 nm.

1,4,5,8-Tetraaminoanthraquinone (Fig. 1b), purified by vacuum sublimation, was deposited onto the PE films heated at a temperature below 80°C in a vacuum of 2.7×10^{-3} Pa. Synthesized indigo (Fig. 1c) and 6,6′-dibromoindigo (Tyrian Purple; Fig. 1d) were also deposited onto the PE films. The prepared specimens were studied using a JEM-2000EX electron microscope.

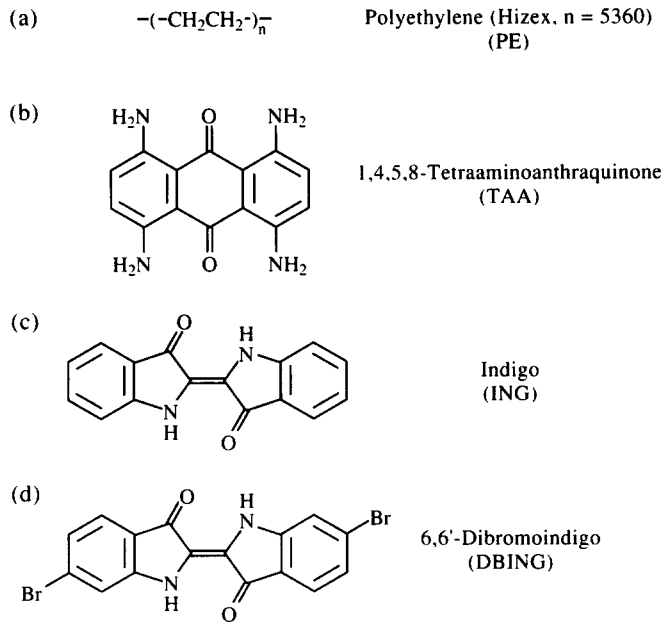

Fig. 1. Molecules of (a) polyethylene, (b) 1,4,5,8-tetraaminoanthraquinone, (c) indigo and (d) 6,6′-dibromoindigo.

RESULTS AND DISCUSSION

The prepared PE films shown in Fig. 2 have the same structure as that described by Kawaguchi *et al.* [7]. They grew in edge-on chain-folded lamellae with the following epitaxial relations with respect to the substrate KCl lattice: $(110)[001]_{PE}//(001)[110]_{KCl}$ and $(110)[001]_{PE}//(001)[\bar{1}10]_{KCl}$, as shown in Fig. 2(c). The lamella looks like a ribbon, elongating perpendicular to the $[001]_{PE}$ direction or along the $[110]_{KCl}$ or $[\bar{1}10]_{KCl}$ axis.

Figure 3(a) shows a transmission electron microscopy (TEM) image of a TAA film 27 nm thick, vacuum-deposited onto the (110) PE substrate. TAA crystals form in thick lamellae or ribbons parallel to the thin, narrow PE ribbons. Reflection spots due to TAA crystals appear in an electron diffraction (ED) pattern in Fig. 3(b), superposed on the spots due to doubly oriented PE films. They indicate the oriented nucleation and growth of TAA crystals with respect to the PE crystals.

An ED pattern in Fig. 4(a) is from an area where the PE ribbons grew mainly along the $[\bar{1}10]_{KCl}$ direction. It simplifies the ED pattern in Fig. 3(b), and the configuration of the reflection spots is schematically shown in Fig. 4(b). Although the crystal structure of TAA has been unknown, the spots

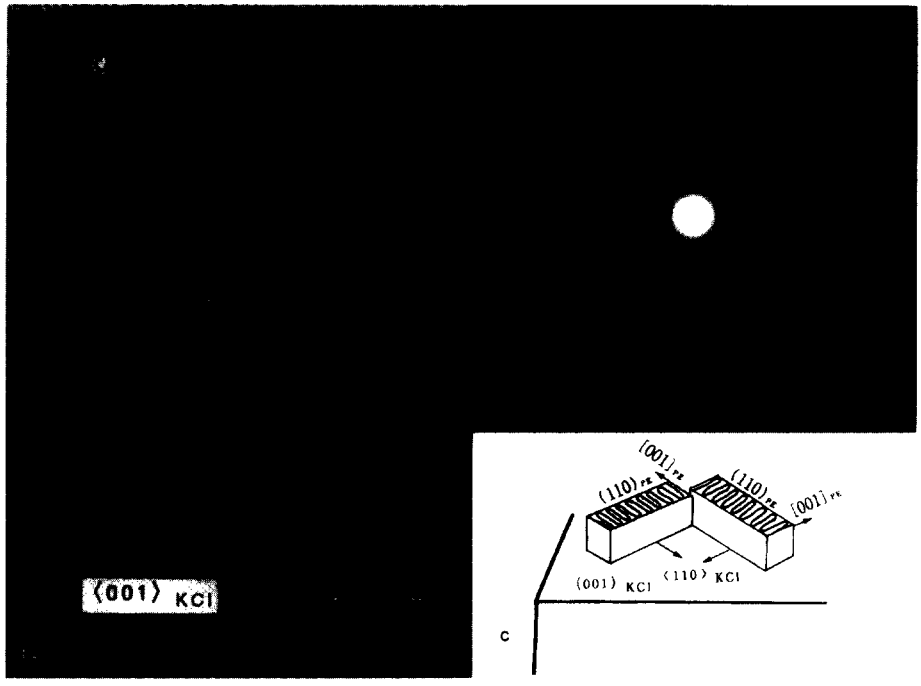

Fig. 2. (a) TEM image of polyethylene (PE) film grown on the (001) surface of KCl from solution. Arrows with c direct the $[001]_{PE}$ axes. (b) ED pattern of the film. (c) Relation between the PE and the KCl substrate.

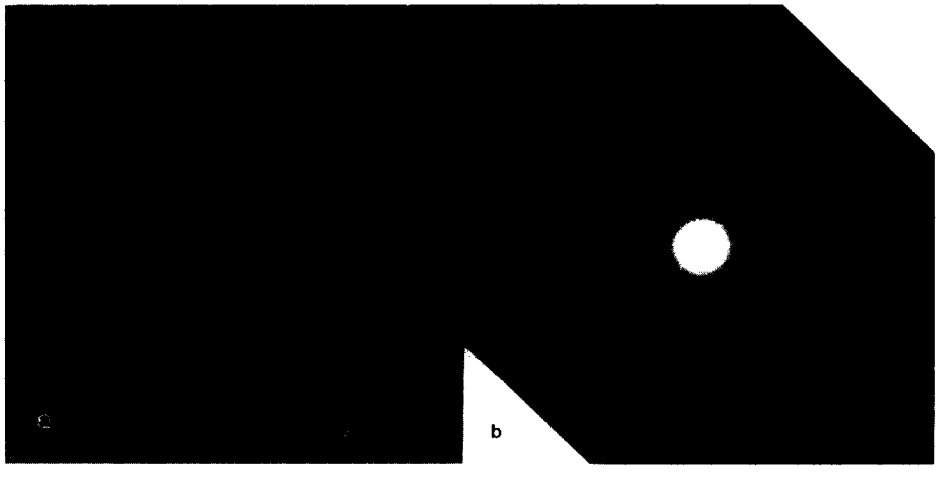

Fig. 3. (a) TEM image of a TAA film vacuum-deposited onto the PE film at 80°C. (b) The corresponding ED pattern.

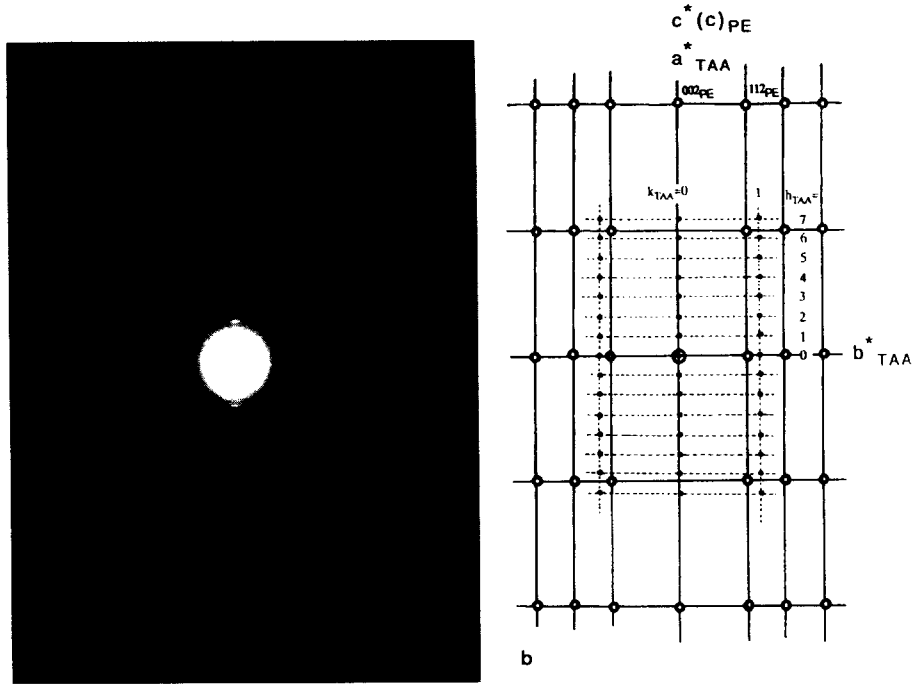

Fig. 4. (a) ED pattern of a TAA film vacuum-deposited onto the PE film. (b) A schematic representation of reflection spots in (a). Open circles represent the PE spots and solid ones the TAA spots.

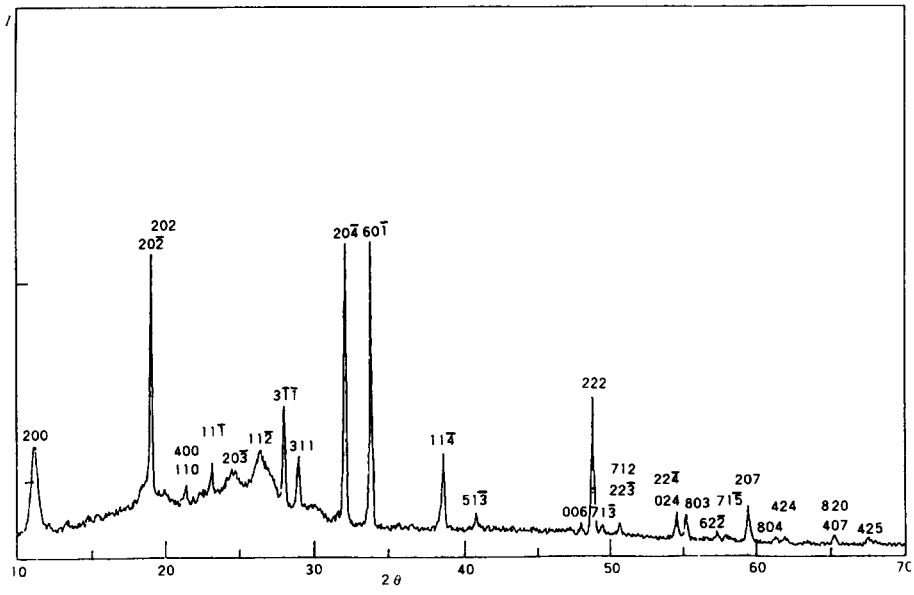

Fig. 5. X-ray diffraction chart of TAA powder used as deposit.

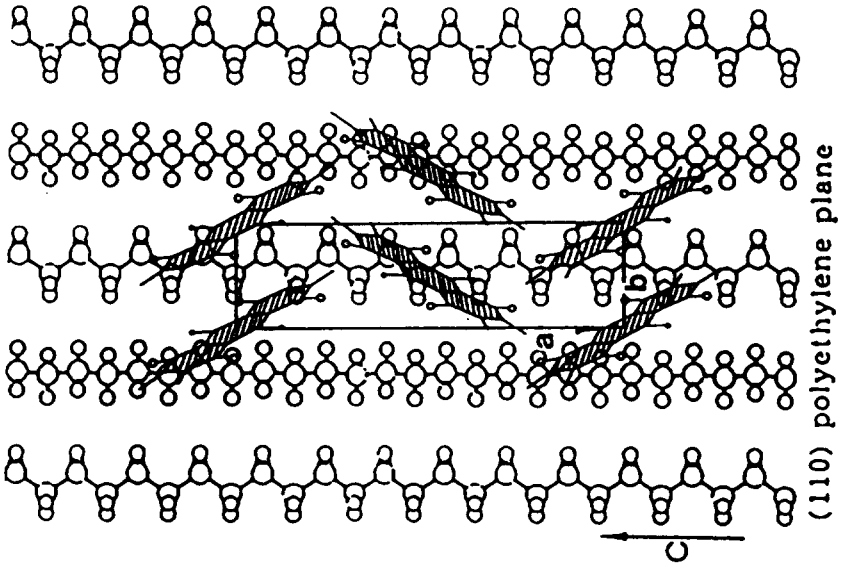

Fig. 6. Molecular configuration of TAA crystal in the epitaxial relation of $(001)[100]_{TAA}//(110)[001]_{PE}$ with respect to the PE substrate, which is projected onto the (110) PE plane.

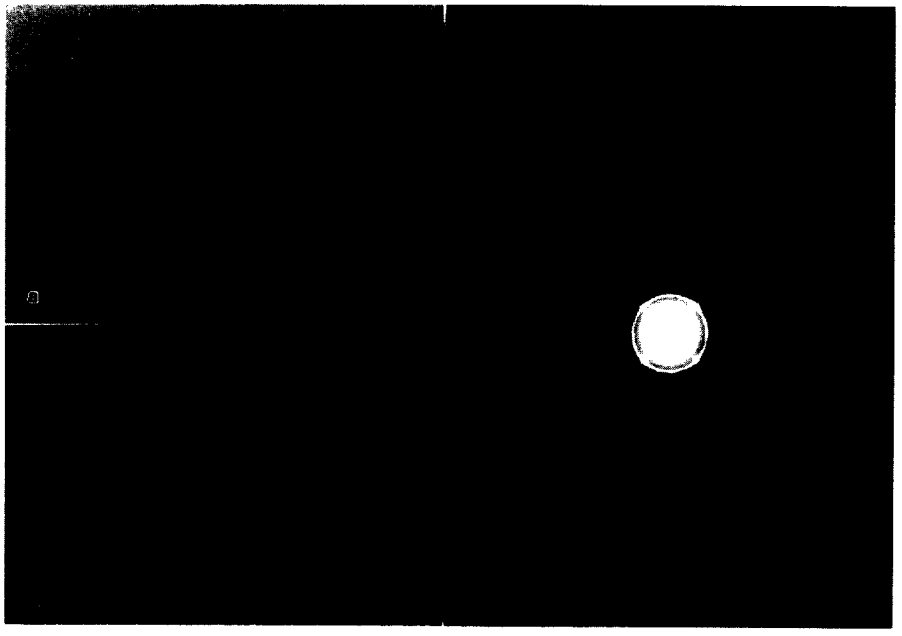

Fig. 7. (a) TEM image of an ING film vacuum-deposited onto the PE film at 70°C. (b) Enlarged image of an area in (a). (c) The corresponding ED pattern.

appearing in Fig. 4(a) indicate reciprocal lattice vectors of $a^* = 1/(1.58\ \text{nm})$ and $b^* = 1/(0.397\ \text{nm})$ and an angle of $\gamma = 90°$ for the TAA crystal. An X-ray diffraction chart of TAA powder used as deposit is shown in Fig. 5. Anthraquinone (AQ) crystal is composed of planar molecules and has the crystal structure of $P2_{1a}$ ($a = 1.5810$, $b = 0.3942$, $c = 0.7865$ nm, $\beta = 102.89°$) [15]. Taking account of the resemblance of TAA to AQ in molecular form, we estimated probable lattice constants of the TAA crystal to be $a = 1.584$ nm, $b = 0.416$ nm, $c = 1.149$ nm and $\beta = 98.03°$, by which the X-ray chart in Fig. 5 was indexed. Consequently, the TAA ribbon crystals, assumed to have the structure of $P2_1a$, nucleate preferentially with the $(001)_{TAA}$ planes parallel to the $(110)_{PE}$ surfaces of the substrate lamellae. The TAA molecules, which have the (211) and $(\bar{2}1\bar{1})$ molecular planes, are adsorbed in edge-standing on the PE surfaces. The $[\bar{1}00]_{TAA}$ axis is the projection of the $[\bar{1}02]_{TAA}$ zone axis of the $(211)_{TAA}$ and $(\bar{2}1\bar{1})_{TAA}$ molecular planes on the PE surface. As a whole the TAA molecules are placed parallel to the PE chains. The TAA crystals then tend to be deposited on the PE crystals with an epitaxial relation of $(001)[100]_{TAA}//(110)[110]_{PE}$, as schematically shown in Fig. 6.

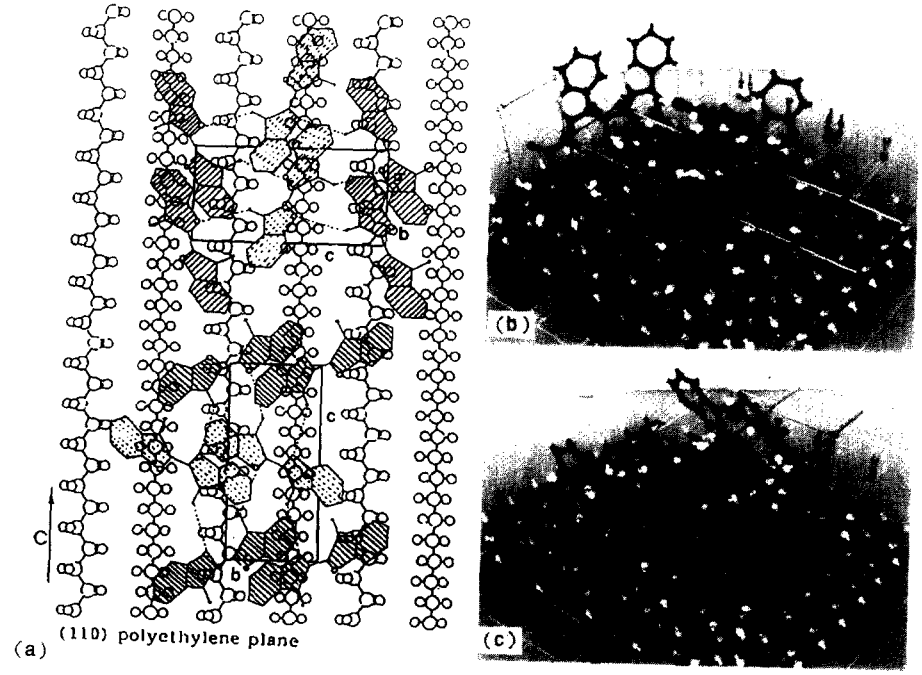

Fig. 8. Molecular configuration of ING crystals in the epitaxial relations of (1) $(\bar{2}01)[010]_{ING}//(110)[110]_{PE}$ and (2) $(\bar{2}01)[010]_{ING}//(110)[001]_{PE}$ with respect to the PE substrate. (a) Projection onto the (110) PE plane. (b,c) Photographs of the models representing relations (1) and (2), respectively.

The double oriented-PE crystals and the TAA crystals grown on their surfaces give rise to the ED pattern shown in Fig. 3(b). TAA ribbons grow, like tangles in sea, along their $[010]_{TAA}$ axes parallel to the $[110]_{PE}$ axis, then stacking their molecular planes nearly perpendicular to the easy growth direction.

A TEM image and its ED pattern of an indigo film 20 nm thick, vacuum-deposited on the PE substrate are reproduced in Fig. 7(a) and 7(b). ING crystals ($P2_1c$; $a=0.924$ nm, $b=0.577$ nm, $c=1.222$ nm, $\beta=117°$) [16] form in thick lamellae or ribbons similar to the TAA crystals. They grow nearly parallel or perpendicular to the thin PE ribbons. The ING crystals extend along the [010] axis with the following preferred orientation with respect to the PE crystal: (1) $(\bar{2}01)[010]_{ING}//(110)[110]_{PE}$ and (2) $(\bar{2}01)[010]_{ING}//(110)[001]_{PE}$ [13].

The molecular configurations postulated for the above orientations (1) and (2) are illustrated in Fig. 8. As seen from the illustration, ING molecules in the $(210)_{ING}$ and $(\bar{2}10)_{ING}$ planes adsorb on the PE substrate with their edges. The zone axis of the $(210)_{ING}$ and $(\bar{2}10)_{ING}$ planes is the $[001]_{ING}$ axis, which is parallel to the $[\bar{1}10]_{PE}$ axis (perpendicular to the PE chains) in orientation (1) and to the $[00\bar{1}]_{PE}$ axis (parallel to the PE chains) in orientation (2). In any case the molecules alternately incline to the inverse directions about the $[001]_{ING}$ axis so that the crystal stands with many crossed feet.

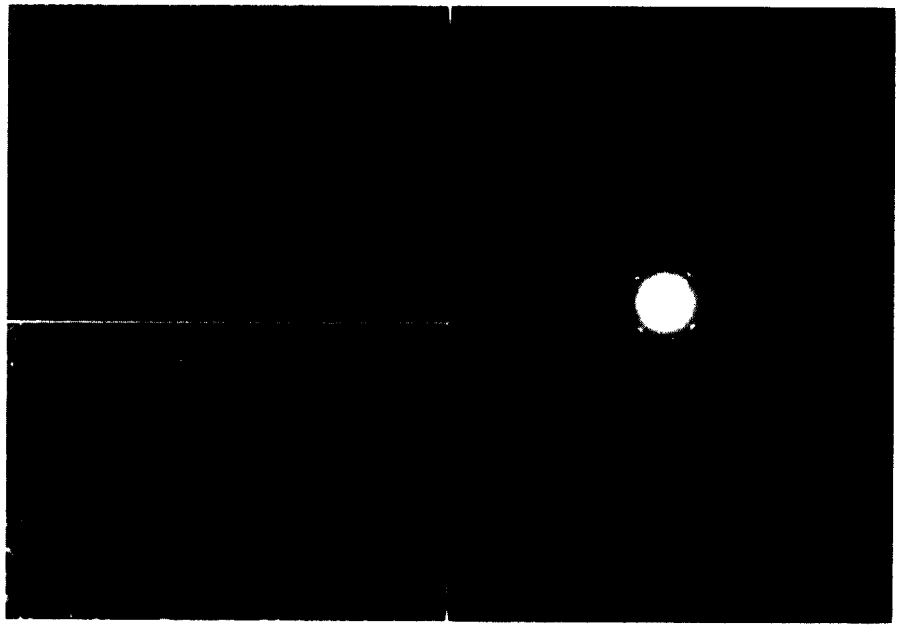

Fig. 9. (a) TEM image of a DBING film vacuum-deposited onto the PE film at 60°C. (b) Enlarged image of an area in (a). (c) The corresponding ED pattern.

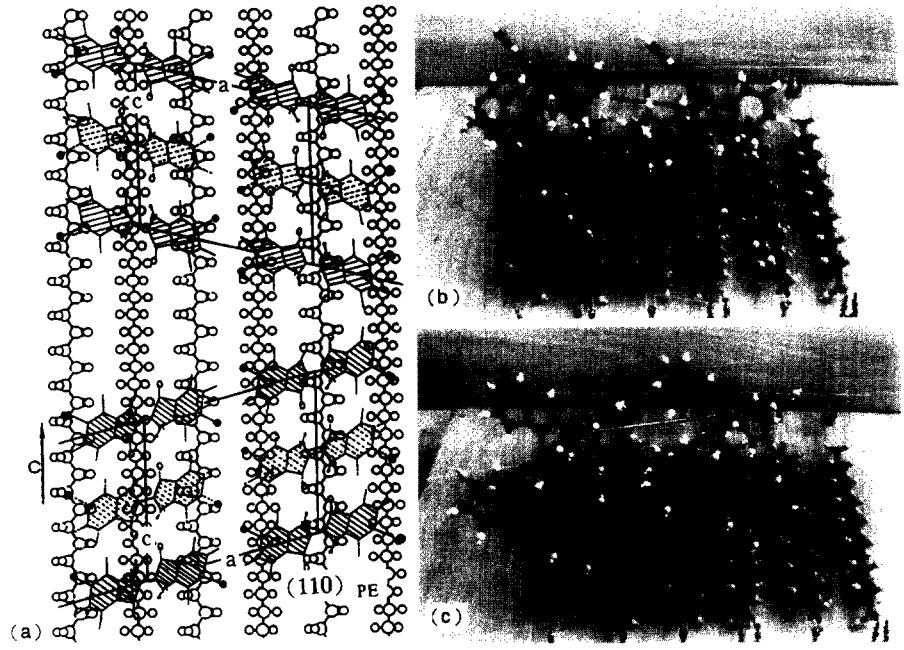

Fig. 10. Molecular configuration of DBING crystals in the epitaxial relations of (1) $(010)[100]_{DBING}//(110)[001]_{PE}$ and (2) $(0\bar{1}0)[100]_{DBING}//(110)[001]_{PE}$ with respect to the PE substrate. (a) Projection onto the (110) PE plane. (b,c) Photographs of the models representing relations (1) and (2), respectively.

Figure 9(a) and 9(b) show TEM images of a dibromoindigo film 10 nm thick, deposited on the PE substrate. DBING crystals ($P2_1a$; $a=1.150$ nm, $b=0.485$ nm, $c=1.260$ nm, $\beta=104.0°$) [17] look like thorns elongating out perpendicular to the PE ribbons. We have found that the DBING crystals grow with preferred orientations of (1) $(010)[100]_{DBING}//(110)[001]_{PE}$ and (2) $(0\bar{1}0)[100]_{DBING}//(110)[001]_{PE}$ on the PE substrate, as shown in Fig. 10 [13]. The DBING crystal also appears as being deposited with many crossed feet on the PE substrate.

A high-resolution TEM image of the DBING film with the PE film is shown in Fig. 11(a), which was taken by a direct magnification of 100 000 with a JEM 2010 microscope operated at 200 kV. Fig. 11(b) and 11(c) show a digitized image, on a computer, of the area indicated by A in Fig. 11(a) and its Fourier-transformed diffractogram. Spots corresponding to the $(002)_{DBING}$ ($d=0.611$ nm), $(200)_{DBING}$ ($d=0.579$ nm) and $(204)_{DBING}$ ($d=0.331$ nm) lattice fringes appear in the diffractogram. Although the PE crystals are so severely damaged by the electron irradiation that spots due to the PE lattice are not observed, the diffractogram indicates that the DBING crystal grows with the $(010)_{DBING}$ plane parallel to the substrate surface, i.e.

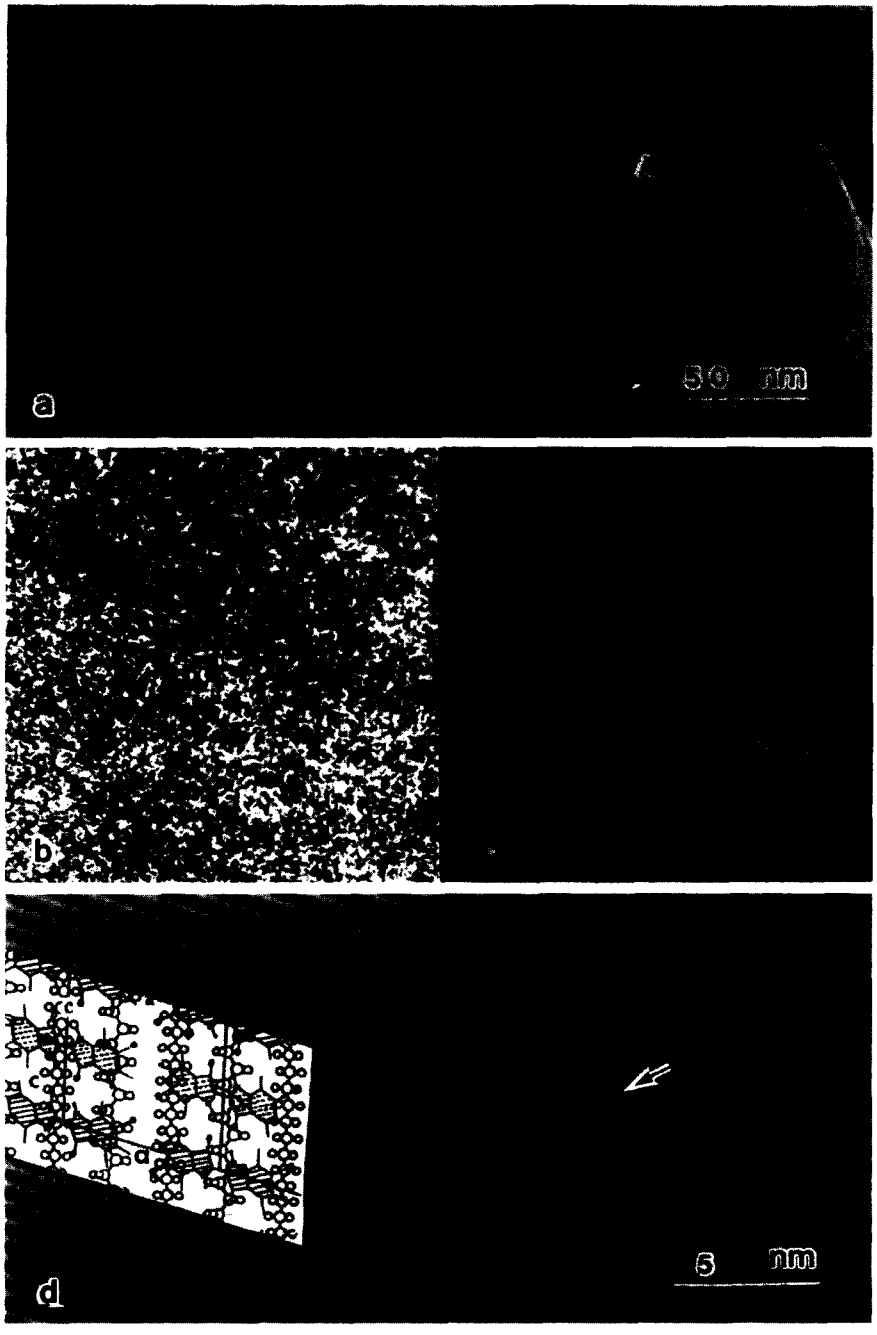

Fig. 11. (a) High-resolution TEM image of a DBING film vacuum-deposited onto the PE film using a minimum dose system. (b) A digitized image of the area indicated by A in (a). (c) A Fourier-transformed diffractogram of the image in (b). (d) A noise-filtered and enlarged image of (b).

TABLE 1
Epitaxy and Growth of Polycyclic Aromatic Dyes on Polyethylene Substrates

Deposit	*Crystal structure and epitaxial relation*	*Growth direction*	*Molecular planes and zone axis of these planes*
TAA	$P2_1a$ $a=1.584$ nm, $b=0.416$ nm $c=1.149$ nm, $\beta=98.03°$ $(001)[100]//(110)[001]_{PE}$	[010]	(211) and $(\bar{2}11)$ $[\bar{1}02]$
ING	$P2_1c$ $a=0.924$ nm, $b=0.577$ nm $c=1.222$ nm, $\beta=117°$ [16] $(\bar{2}01)[010]//(110)[110]_{PE}$ and $(\bar{2}01)[010]//(110)[001]_{PE}$	[010]	(210) and $(\bar{2}10)$ [001] along $[00\bar{1}]_{PE}$ or $[\bar{1}10]_{PE}$
DBING	$P2_1a$ $a=1.150$ nm, $b=0.485$ nm $c=1.260$ nm, $\beta=104°$ [17] $(010)[100]//(110)[001]_{PE}$ and $(0\bar{1}0)[100]//(110)[001]_{PE}$	[010]	(011) and $(0\bar{1}1)$ [100] along $[001]_{PE}$

in the above orientation of (1). A processed image, noise-filtered and enlarged is shown in Fig. 11(d), with the structure model. It exhibits definitely the $(002)_{DBING}$ fringes, in which the lattice distortion and dislocations (indicated by an arrow head) can be seen.

In conclusion, the epitaxy and growth behaviour of these polycyclic dye crystals on the (110) PE crystal are summarized in Table 1. As indicated by the ED patterns, which include the ring component, all the crystals do not grow completely with epitaxy. The epitaxy, however, implies an appreciable interaction between the dye molecules and PE fibres.

ACKNOWLEDGEMENTS

We wish to express our thanks to Dr Y. Yabuuchi, Matsushita Tecnoresearch Inc., and Professor Y. Shibahara, Kyoto University of Education, for helping in the X-ray experiment, and to Mr M. Kawasaki, JEOL Co., and Mr Isshiki, Kyoto Institute of Technology, for high-resolution electron microscopy in Fig. 11. We also thank Dr T. Torimoto, Osaka Scientific Education Center, for providing DBING samples used in the present experiment.

REFERENCES

1. Richards, R. B., *Journal of Polymer Science*, **6** (1951) 397.
2. Kobayashi, K. and Takahashi, T., *Kobunshi Kagaku*, **28** (1971) 178.

3. Takahashi, T., Inamura, M. and Tsujimoto, I., *Kobunshi Kagaku*, **28** (1971) 973.
4. Takahashi, T., Inamura, M. and Tsujimoto, I., *Kobunshi Kagaku*, **28** (1971) 978.
5. Willems, J., *Kolloid-Z. und Z. Polymere*, **251** (1973) 496.
6. Kawaguchi, A., Okihara, T., Ohara, M., Tsuji, M. and Katayama, K., *Journal of Crystal Growth*, **94** (1989) 857.
7. Kawaguchi, A., Okihara, T. and Katayama, K., *Journal of Crystal Growth*, **99** (1990) 1028.
8. Okihara, T., Kawaguchi, A., Ohara, M. and Katayama, K., *Journal of Crystal Growth*, **106** (1990) 318.
9. Okihara, T., Kawaguchi, A., Ohara, M. and Katayama, K., *Journal of Crystal Growth*, **106** (1990) 333.
10. Kawaguchi, A., Okihara, T., Murakami, S., Ohara, M. and Katayama, K., *Journal of Polymer Science, Part B: Polymer Physics*, **29** (1991) 683.
11. Wittmann, J. C. and Smith, P., *Nature*, **352** (1991) 414.
12. Ueda, Y., Kuriyama, T., Hirai, T. and Ashida, M., *Journal of Electron Microscopy*, **43** (1994) 99.
13. Tanabe, K. and Shiojiri, M., *Journal of Crystal Growth*, **166** (1996) 935.
14. Fischer, E. W., *Kolloid-Z.*, **159** (1958) 108.
15. Lonsdale, K., Milledge, H. J. and Sayed, K. E., *Acta Crystallographica*, **20** (1966) 1.
16. Von Eller, H., *Mémoires Présents a la Société Chimique*, **5** (1955) 1433.
17. Süsse, P. and Krampe, C., *Naturwissenschaften*, **66** (1979) 110.